Detection of Apoptotic Cells

Cells were cultured on 8-well Lab-Tek chamber slides with or without elcatonin. Apoptotic cells were detected by rhodamine fluorescence using an ApopTag Red In Situ Apoptosis Detection Kit (Chemicon, Temecula, CA, http://www.chemicon.com).

RNA Extraction and Reverse Transcription-Polymerase Chain Reaction

Total RNA was extracted from sorted or cultured cells with a Qiagen RNeasy Mini kit according to the manufacturer's instructions (Qiagen, Hilden, Germany, http://www1.qiagen.com) and then reverse-transcribed into cDNA by using TaqMan Reverse Transcription Reagents (Roche). The polymerase chain reaction (PCR) was performed with cDNA products under the following cycling conditions: 94°C for 3 minutes followed by 30–40 cycles of amplification, annealing, and extension (94°C for 15 seconds, 58°C for 30 seconds, and 72°C for 30 seconds) with a final incubation at 72°C for 5 minutes. Specific primer sequences used for PCR are described in supplemental online Materials and Methods.

Target Synthesis, Gene Chip Hybridization, and Data Acquisition

To label antisense RNA (aRNA) with biotin for microarray hybridization, we followed the protocol supplied by the manufacturer (Affymetrix, Santa Clara, CA, http://www.affymetrix.com). Because the starting amount of total RNA was 100 ng for the sorted SM/C-2.6$^+$ cell fraction, we used a two-cycle biotin aRNA synthesis kit (Affymetrix). Labeled aRNA was fragmented according to Affymetrix GeneChip protocol and then hybridized to Affymetrix MOE430A GeneChip arrays for 16 hours. After washing, the gene chips were stained according to the instrument's standard Eukaryotic GE WS2v4 protocol using antibody-mediated signal amplification. The signal was determined, using the Microarray Suite (MAS) 5.0 absolute analysis algorithm, as the average fluorescence intensity among the intensities obtained from the probe set. The signal of a probe set was calculated as the one-step biweight estimate of combined differences of all the probe pairs (perfectly matched and mismatched) in the probe set. A one-sided Wilcoxon's signed rank test was used to calculate a p value that reflects the significance of differences between perfectly matched and mismatched probe pairs. The p value was used to make the absolute call for probe sets. A "Present" call was assigned to transcripts for p values between 0 and .04, a "Marginal" call was assigned to transcripts for p values between .04 and .06, and an "Absent" call was assigned to transcripts for p values between .06 and 1.0.

Microarray Data Analysis

Scanned output files were analyzed by the probe level analysis package MAS 5.0 (Affymetrix). The Present/Absent call provided by the Affymetrix programs was used for the first selection. The MAS 5.0-generated raw data were uploaded to GeneSpring software version 7.0 (Silicongenetics, Redwood, CA, http://www.chem.agilent.com/scripts/PHome.asp). Data normalization was achieved by one of two methods: (a) each signal was divided by the 50th percentile of all signals in a specific hybridization experiment or (b) each signal was divided by the median of its values in all samples. A more reliable list of "5-fold changing" genes was obtained by applying the filtering options of GeneSpring. Present calls in all (four) quiescent or activated satellite cell probes were selected and a restriction, which passed genes with raw data above 100, was applied. Then, using all the quiescent and activated satellite cells as data, we performed a one-way analysis of variance test between the quiescent satellite cell group and the activated satellite cell group. In particular, a parametric test, with variances assumed equal (Student's t test, p value cut-off .05; multiple testing correction: Benjamini and Hochberg false discovery rate), was applied. The genes passing all these filters and tests were selected as "5-fold changing genes." Nonmyogenic cells (SM/C-2.6$^-$/CD45$^-$ cells) were also prepared four times.

Gene Set Enrichment Analysis

GSEA [22] is a statistical analysis of sets of gene expression profiles, separated by phenotypic labels. Using GSEA, we can test hypotheses concerned with predefined sets of genes; the rank orderings of the genes in the whole gene set calculated with a given ranking method are random with regard to a given classification of samples. As a result of the analysis, nominal p values, family-wise error rate p values, and false discovery rate (FDR) q values for test hypotheses (thus for gene sets) were obtained.

In our analysis, we used the GSEA-P software package [22], which is available from the Broad Institute (Cambridge, MA, http://www.broad.mit.edu). We prepared, as input to the GSEA-P, the MAS 5.0-generated raw signal data and gene sets derived independently. We chose genes on the chip that were detected (the Present call was assigned) in at least one sample (17,150 of 22,626). The raw signals of the chosen genes were normalized so that their total sum was 1. Because the total amount of mRNA in a quiescent satellite cell (QSC) is much less than that in an activated satellite cell (ASC), the normalized signal should be understood as a relative signal among the chosen genes. To compile the gene sets, we assigned each probe to a gene ontology (GO) category [23] using annotations of the MOE430A chip (September 22, 2005) provided by Affymetrix. Therefore, these gene sets reflect the structure of the GO categories and subcategories of molecular function (MF), biological process (BP), and cellular component (CC). The 17,150 genes chosen comprised 1,674, 1,698, and 412 gene sets in the MF, BP, and CC subcategories, respectively, and were reduced to 162, 218, and 85 after filtering out gene sets with sizes smaller than 20 or larger than 1,000. We ran the GSEA-P with the signal-to-noise option for its ranking metric, with permutation over phenotype labels of QSC and ASC samples, and repeated it 2,000 times with the "weighted" option for its scoring scheme.

Results and Discussion

Isolation of Quiescent Satellite Cells from Mouse Skeletal Muscle

First, to obtain RNA samples for microarray analysis, we prepared mononuclear cells from 8- to 12-week-old C57BL/6 mouse muscle, and the SM/C-2.6$^+$ fraction was collected as the satellite cell fraction by FACS [18] (Fig. 1A). Consistent with our previous report, more than 97% of fresh SM/C-2.6$^+$ cells expressed Pax7 (Fig. 1B) but were mostly negative for both MyoD (Fig. 1Ca, 1Cb) and Ki67 (Fig. 1Ce, 1Cf). After 4–5 days of culture, more than 98% of SM/C-2.6$^+$ cells expressed MyoD (Fig. 1Cg, 1Ch) and Ki67 (Fig. 1Ck, 1Cl). Both freshly isolated, uncultured SM/C-2.6$^+$ cells and SM/C-2.6$^+$ cells cultured in growth medium were negative for myogenin expression (Fig. 1Cc, 1Cd, 1Ci, 1Cj), but these cells started to express myogenin and differentiated well into multinucleated myotubes after mitogen withdrawal (data not shown). In contrast, more than 99% of freshly isolated SM/C-2.6$^-$/CD45$^-$ cells were negative for Pax7 expression (Fig. 1Bc, 1Bd), and cultured SM/C-2.6$^-$/CD45$^-$ cells did not express MyoD (data not shown), again indicating that myogenic cells are highly enriched in the SM/C-2.6$^+$ fraction.

The forward and side scatter profiles of freshly isolated SM/C-2.6$^+$ cells showed that they are small and uniform in granularity (data not shown). In fact, as shown in Figure 1D, the cell size of fresh SM/C-2.6$^+$ cells was estimated to be approximately one-half that of cultured SM/C-2.6$^+$ cells based on the forward scatter profile, indicating that the freshly isolated SM/C-2.6$^+$ cells were not activated yet. Pyronin Y staining showed the small amount of RNA content in freshly isolated SM/C-2.6$^+$ cells (Fig. 1D). In general, a Pyronin^{low} and Hoechst 33342^{low} fraction is considered

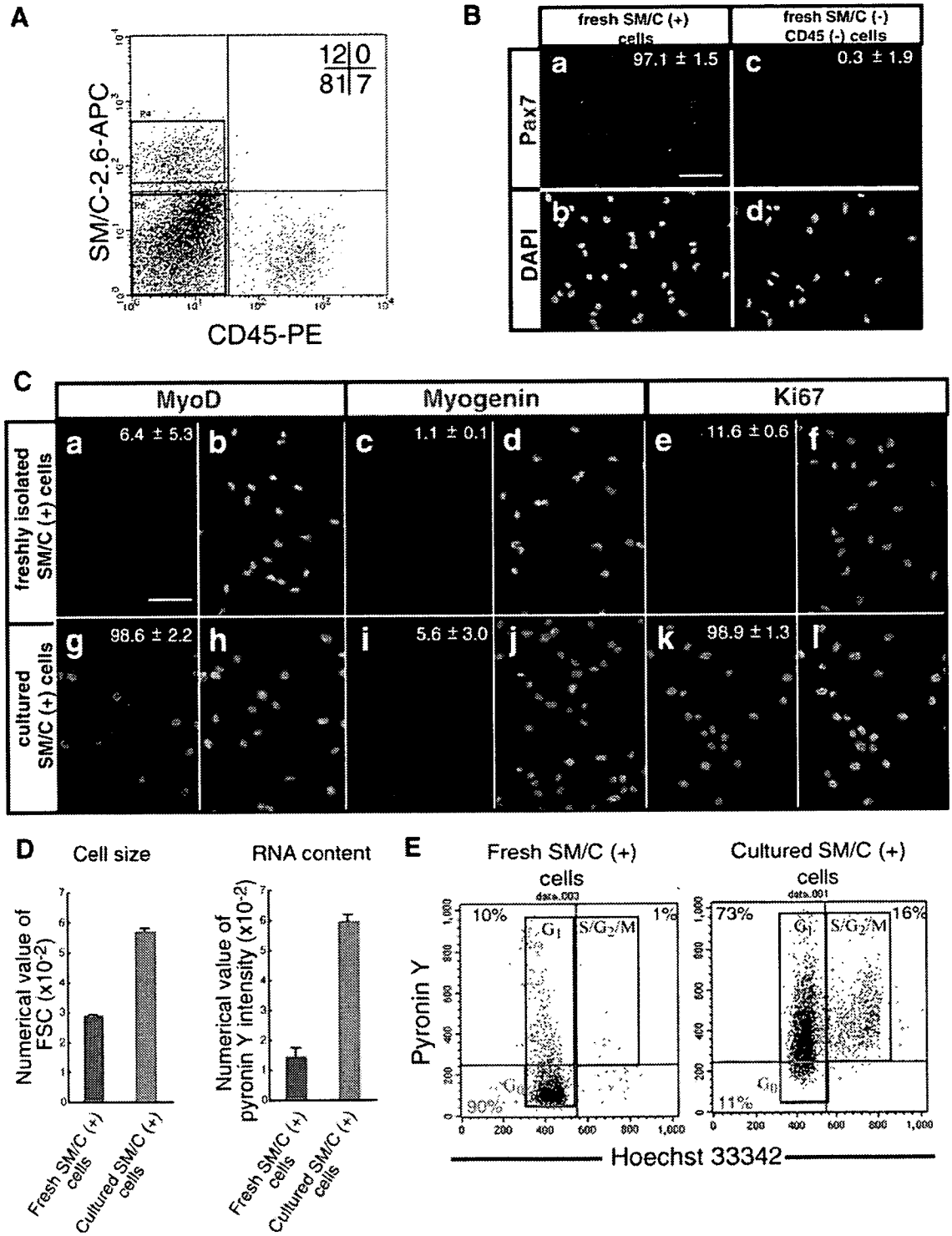

Figure 1. SM/C-2.6$^+$ cells isolated from skeletal muscle by fluorescence-activated cell sorting (FACS) are highly purified quiescent satellite cells and proliferate and express MyoD in culture. **(A):** Mononucleated cells prepared from uninjured limb muscles of adult mice were stained with anti-CD45 antibody and SM/C-2.6 monoclonal antibody. The SM/C-2.6$^+$ fraction (red square) and the SM/C-2.6$^-$/CD45$^-$ fraction (blue square) were collected for further analysis. **(B):** Freshly isolated SM/C-2.6$^+$ and SM/C-2.6$^-$/CD45$^-$ cells were stained with anti-Pax7 **(Ba, Bc)** antibody and DAPI **(Bb, Bd)**. The percentages of Pax7-positive cells in each cell fraction are shown. Cell fractionation was performed three times, and more than 300 cells from each fraction were counted. Scale bar: 50 μm. **(C):** Freshly isolated SM/C-2.6$^+$ cells and SM/C-2.6$^+$ cells cultured for 4 days in the presence of basic fibroblast growth factor were stained with antibodies to MyoD **(Ca, Cg)**, myogenin **(Cc, Ci)**, or Ki67 **(Ce, Ck)**. Percentages of MyoD-, myogenin-, or Ki67-positive cells are shown. Cell fractionation was performed three times, and more than 180 cells were counted each time. Nuclei were stained with DAPI **(Cb, Cd, Cf, Ch, Cj, Cl)**. Scale bar: 50 μm. **(D):** The mean value of FSC (cell size) and Pyronin Y intensity (RNA content) of freshly isolated SM/C-2.6$^+$ cells and satellite cells cultured in vitro. The value is an average of two independent experiments. **(E):** The percentages of cells in the G0 phase of the cell cycle were estimated by staining with Pyronin Y and Hoechst 33342. The number in the lower left of each FACS profile indicates the percentage of the G0 cells: 90% for fresh SM/C-2.6$^+$ cells and 11% for cultured SM/C-2.6$^+$ cells. Abbreviations: APC, allophycocyanin; DAPI, 4,6-diamidino-2-phenylindole; FSC, forward scatter; M, mitosis phase; PE, phycoerythrin; S, synthesis phase.

to be G0 cells [24]. Pyronin Y and Hoechst double staining shows that approximately 90% of fresh SM/C-2.6$^+$ cells were in the G0 phase of the cell cycle. In contrast, 90% of cultured SM/C-2.6$^+$ cells were cycling (Fig. 1E).

Thus, our procedure, which takes 5–6 hours in total to isolate 1–2 × 10^5 SM/C-2.6$^+$ cells from one C57BL/6 mouse, enables us to isolate satellite cells still in a quiescent and undifferentiated state. The yield corresponds to 10%–15% of the total mononucleated cells obtained from mouse hind limb muscles by enzymatic digestion. Therefore, in this report, we call freshly isolated SM/C-2.6$^+$ cells "quiescent satellite cells" and cultured, proliferating SM/C-2.6$^+$ cells "activated satellite cells." Our procedure was also applicable to dystrophin-deficient *mdx* muscle with modifications, although 30%–40% of *mdx* satellite cells are Ki67-positive (M. Ikemoto et al., submitted manuscript). Unfortunately, SM/C-2.6 did not react with satellite cells from dystrophin-deficient dystrophic dogs (data not shown).

Single Gene Analysis of Quiescent and Activated/Proliferating Satellite Cells

We prepared RNA samples from quiescent satellite cells and activated satellite cells and performed microarray analysis using Affymetrix GeneChips. Hybridization and data collection were performed four times using independent preparations of cells and RNA samples for each cell fraction. Raw data are available at http://www.ncbi.nlm.nih.gov/geo. The Gene Expression Omnibus accession number is GSE3483.

First, we compared the expression levels of individual genes in quiescent and activated states using GeneSpring software. We found that 507 genes (665 probes) were expressed in quiescent satellite cells at more than fivefold higher levels than in activated satellite cells (Fig. 2A). We roughly categorized these 507 genes into 11 gene groups: cell adhesion (15 genes), cell cycle regulation (26), proteolysis (21), cytoskeleton (13), cell surface (41), extracellular (61), immunoresponse (22), signal transduction (81), transcription (67), transport and metabolism (82), and unknown (78) based on Gene Ontology and listed all of them in supplemental online Table 1. On the other hand, 659 genes (814 probes) were upregulated (>fivefold) in the activated state (supplemental online Table 2). We also examined the gene expression of proliferating satellite cells/myoblasts in vivo that were directly isolated from regenerating muscle 2 days after cardiotoxin injection. The activated and proliferating satellite cells in vivo showed an expression profile quite similar to satellite cells cultured in vitro (data not shown).

Upregulation of Cell Cycle Regulators in Quiescent Satellite Cells

Under normal conditions, most satellite cells are in the G0 phase of the cell cycle, possibly preventing their premature exhaustion. It is of note that nine genes encoding negative regulators of the cell cycle were highly upregulated in the quiescent stage: *Rgs2* (*regulator of G-protein signaling 2*) (×69, ×23), *Rgs5* (×37, ×21), *Pmp22* (*peripheral myelin protein 22*)/*Gas3* (growth arrest specific 3) (×25), *Cdkn1c* (cyclin-dependent kinase inhibitor 1C)/*p57* (×14), *Spry1* (sprouty homolog 1) (×11), *Gas1* (×7, ×6), *Reck* (reversion-inducing-cysteine-rich protein with kazal motifs) (×6), *Ddit3* (DNA-damage inducible transcript 3) (×6), and *Trp63* (transformation-related protein 63) (×5) (supplemental online Table 1). Reverse transcription (RT)-PCR confirmed that *Rgs2*, *Pmp22*, *p57*, and *Spry1* are highly expressed in quiescent satellite cells and downregulated in activated satellite cells (Fig. 2Ba).

Cyclin-dependent kinase inhibitors (CKIs) play a key role in controlling the cell cycle in many cell types. p21 (CIP1) triggers the cell cycle exit of proliferating myoblasts to initiate myoblast terminal differentiation in response to differentiation signals [25]. p57 (KIP2) is induced in myoblasts upon differentiation. Gene targeting experiments showed that these two CKIs redundantly control cell cycle exit during myogenesis [26]. Compared with irreversible cell cycle arrest upon differentiation, however, attainment of a reversible G0 state by satellite cells is poorly understood. In vitro studies suggested that Rb family members p130 and p27 are involved in the reversible cell cycle exit of proliferating myoblasts to return satellite cells to quiescence [16]. In our experiments, p21 (×0.5), p27 (×1.5), and p130 (×2–3) were not significantly upregulated in quiescent satellite cells. Reflecting the levels of p57 mRNA, p57 protein was found in more than 90% of freshly isolated SM/C-2.6$^+$ cells (Fig. 2Ca). Whether p57 is required for acquisition and maintenance of quiescence of satellite cells remains to be determined in a future study.

Upregulation of Myogenic Inhibitors in Quiescent Satellite Cells

Quiescent satellite cells barely express myogenic basic helix-loop-helix (bHLH) factors. Activity of the *Myf-5* locus was revealed through a reporter gene, but Myf-5 protein is hardly detected in dormant satellite cells. On activation, satellite cells upregulate Myf5 and start to express MyoD [27] (Fig. 1). Our microarray analyses revealed that several myogenic inhibitory molecules were upregulated in quiescent satellite cells: *Bmp6* (*bone morphogenetic protein 6*) (×214), *Bmp4* (×66), *Bmp2* (×82), *Heyl* (*hairy/enhancer-of-split related with YRPW motif-like*)/*Herp3*/*Hrt3*/*hesr3* (×101, ×33, ×32), *Musculin*/*MyoR* (×83), *Notch3* (×9). Upregulation of *Bmp4*, *Bmp6*, *Msc*/*MyoR*, and *Heyl* in quiescent satellite cells was confirmed by RT-PCR (Fig. 2Bb). BMP4 is reported to negatively regulate MyoD expression in somite myogenesis [28] and differentiation of satellite cells, where BMP4-induced inhibition of myogenic differentiation requires Notch signaling [29]. Notch signaling is reported to inhibit the differentiation of myoblasts by repression of MyoD expression [30]. In postnatal muscle, Notch signaling controls satellite cell activation and their cell fate [31], and insufficient upregulation of the Notch ligand Delta is casually related to impaired regeneration of aged muscle [32]. Among several molecules in the Notch signaling pathway, our microarray analysis showed that *Notch3* and one of the Notch-effector genes, *Heyl*, are highly expressed in quiescent satellite cells. When cross-sections of normal mouse tibialis anterior (TA) muscle were stained with specific antibodies, HeyL was found in nearly all Pax7-positive nuclei, and Notch3 was expressed on the surface of mononuclear cells beneath the basal lamina (Fig. 2Cb, 2Cc). These results suggest that Notch3 and HeyL play roles in Notch signaling to inhibit muscle differentiation of satellite cells. Musculin/MyoR is a bHLH transcription factor originally cloned as a repressor of MyoD [33]. Musculin-null mice do not exhibit any skeletal muscle defect, but musculin is likely to negatively regulate MyoD in muscle regeneration [34].

In addition to negative regulators, two positive regulators of myogenesis, *Gli2* (*GLI-Kruppel family member GLI2*) (×29, ×13) and *Meox2* (*mesenchyme homeobox 2*) (×17), are preferentially expressed in quiescent satellite cells. Gli2 directly upregulates Myf5 [35], and Meox1 and 2 regulate Pax3 and Pax7 expressions [36]. These observations suggest that Gli2 and Meox2 maintain lineage identity in quiescent satellite cells.

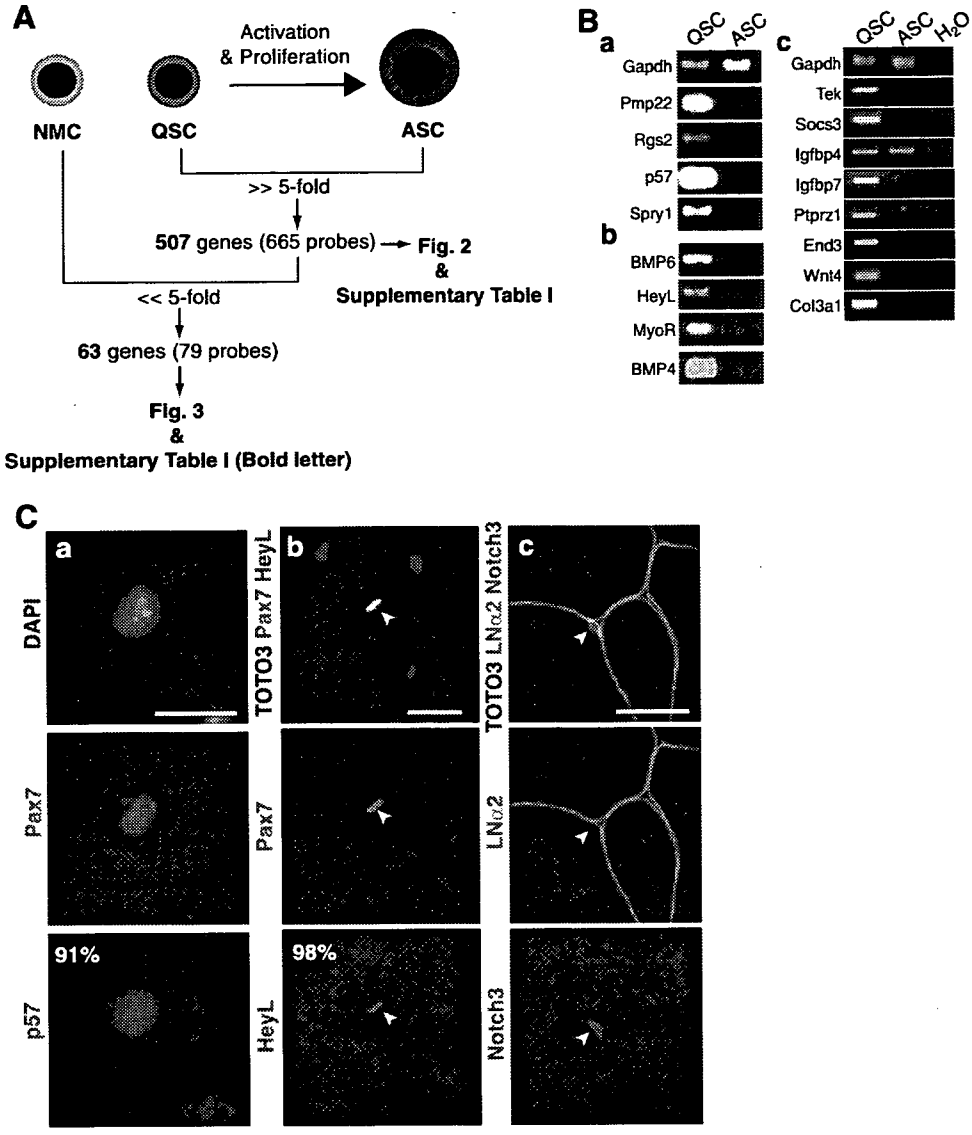

Figure 2. Identification of the genes expressed at higher levels in QSC than in ASC. **(A):** Outline of gene expression analysis at single gene level. Sixty-three genes out of 507 genes were found to be expressed at a higher level (more than fivefold) in quiescent satellite cells than in NMC. We applied Student's *t* test (p value .05) with multiple testing corrections (Benjamini and Hochberg false discovery rate). **(B):** Reverse transcription-polymerase chain reaction of eight relevant genes involved in cell cycle regulation **(Ba)**, inhibition of myogenesis **(Bb)**, or other biological process **(Bc)** (Table 1). Total RNAs were isolated from fluorescence-activated cell sorting-sorted SM/C-2.6$^+$ cells (QSC) and cultured SM/C-2.6$^+$ cells (ASC). *Gapdh* is control. **(Ca):** Mononucleated cells from intact skeletal muscle were stained with anti-p57 (red), Pax7 (green), and DAPI (blue) immediately after sorting. **(Cb, Cc):** Cross-sections of normal skeletal muscle were stained with antibodies to HeyL (red in **[Cb]**), Notch3 (red in **[Cc]**), Pax7 (green in **[Cb]**), or laminin α2 chain (green in **[Cc]**). More than 90% of Pax7-positive cells were positive for p57. Nearly all Pax7-positive cells expressed HeyL. Notch3 was expressed on the cell surface on satellite cells. Nuclei were stained with TOTO3 (blue). Scale bar: 20 μm. Abbreviations: ASC, activated satellite cells; DAPI, 4,6-diamidino-2-phenylindole; LNα2, laminin α2; NMC, nonmyogenic cells; QSC, quiescent satellite cells.

Identification of Quiescent Satellite Cell-Specific Genes

To identify quiescent satellite cell-specific genes from 507 genes (Fig. 2A), we next prepared RNA samples from nonmyogenic cells (SM/C-2.6$^-$/CD45$^-$ in Fig. 1A) and performed microarray analysis using Affymetrix GeneChips. Statistical analysis validated that 63 genes out of 507 genes were preferentially expressed (>fivefold) in quiescent satellite cells compared with nonmyogenic cells or activated satellite cells (genes in bold letters in supplemental online Table 1).

To confirm the microarray results, we next performed RT-PCR on 14 genes of interest. In addition to microarray samples, the results for TA muscle and a myogenic cell line, C2C12 cells, are also shown (Fig. 3). Two well-established satellite cell markers (Pax7 and M-cadherin) were expressed not only in quiescent satellite cells but also in activated satellite cells and/or C2C12 cells. In contrast, two cell surface molecules, Odz4, a mouse homolog of the *Drosophila* pair-rule gene *Odd Oz* [37], and CTR, a signaling molecule Tribbles1, and two extracellular molecules, endothelin3 and chordin-like2, were all confirmed to be expressed exclusively in quiescent satellite cells.

Gene Set Enrichment Analysis Revealed Gene Groups Upregulated in Quiescent Satellite Cells

Single-gene analysis permitted us to identify candidate genes that regulate quiescence and undifferentiated state of satellite cells in vivo. To complement the analysis at the single gene

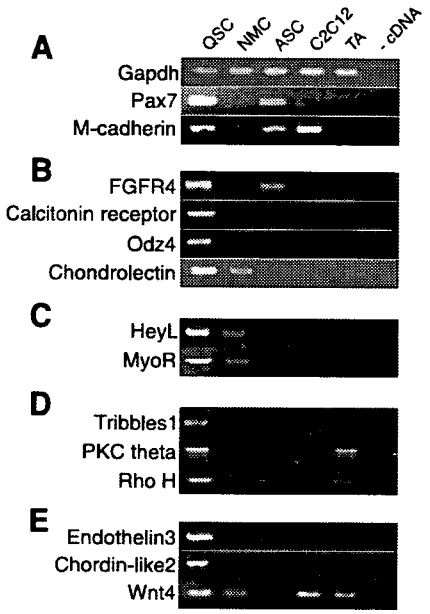

Figure 3. Reverse transcription-polymerase chain reaction (RT-PCR) of quiescent satellite cell-specific genes. Expression levels of quiescent satellite cell-specific genes in fluorescence-activated cell sorting-sorted SM/C-2.6$^+$ cells (lane 1), SM/C-2.6$^-$/CD45$^-$ non-myogenic cells (lane 2), cultured SM/C-2.6$^+$ cells (lane 3), C2C12 cells (lane 4), and TA muscle (lane 5) were confirmed by RT-PCR. The genes are categorized into five groups: well-known satellite cell markers (**A**), cell surface receptors (**B**), transcription factors (**C**), signal molecules (**D**), and extracellular molecules (**E**). Lane 6 is the reaction without cDNA templates. Abbreviations: ASC, activated satellite cells; NMC, nonmyogenic cells; QSC, quiescent satellite cells; TA, tibialis anterior.

level, we performed gene set enrichment analysis [22]. GSEA is an analytical method that identifies small but coordinated changes of predefined gene sets but not up- or downregulation of individual genes, which therefore would help us to identify important signaling pathways or regulatory mechanisms for satellite cells. We used GO annotations [23] to group all genes on GeneChips and tried to extract gene sets that are upregulated as a whole in quiescent satellite cells compared with activated and proliferating satellite cells (Fig. 4). When all genes were categorized into 1,674 gene sets according to their biological process ontology, only three gene sets were judged to be coordinately upregulated in quiescent satellite cells (FDR < 0.25): cell-cell adhesion, regulation of cell growth, and transmembrane receptor protein tyrosine phosphatase signaling pathway (Table 1). When all genes were grouped into 1,698 gene sets according to cellular component ontology, three gene sets, insoluble fraction, extracellular region, and collagens, were found to be coordinately upregulated in quiescent satellite cells compared with activated/proliferating satellite cells (Table 1). When grouped into 412 gene sets based on their predicted molecular functions, three gene sets, extracellular matrix structural constituent conferring tensile strength, copper ion binding, and lipid transporter activity, were found to be coordinately upregulated in quiescent satellite cells (Table 1). Seven genes listed in Table 1 (*Tek, Socs3, Igfbp7, Ptprz1, End3, Wnt4,* and *Col3a1*) were confirmed to be upregulated in quiescent satellite cells by RT-PCR (Fig. 2Bc). A more detailed discussion on GSEA results is in the supplemental online Discussion.

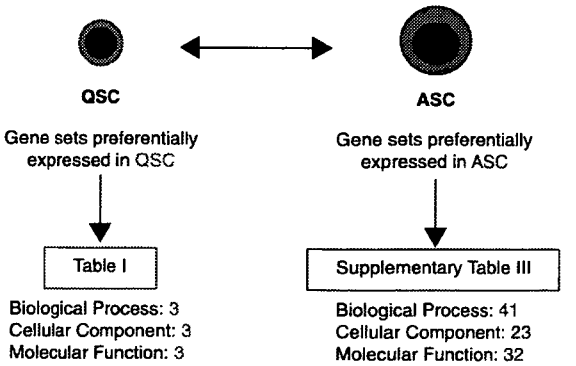

Figure 4. Gene set enrichment analysis (GSEA) of quiescent and activated satellite cells. Summary of GSEA comparing QSC with ASC using gene sets based on three major Gene Ontology trees: cellular component, biological process, and molecular function. Gene sets with high enrichment score (1 − [false discovery rate q value] are >0.75) are listed in Table 1 and supplemental online Table 3. Abbreviations: ASC, activated satellite cells; QSC, quiescent satellite cells.

Gene Sets That Are Coordinately Upregulated upon Activation

Many gene sets were found to be coordinately upregulated in activated/proliferating satellite cells compared with quiescent satellite cells (Fig. 4). These are involved in active synthesis of DNA, RNA and protein, progression of cell cycle (*Cdc2a, Cdc20, Cdc25c, Ccnb1, Ccna2,* etc.), mitochondrial activities, and so on. The gene sets are all listed in supplemental online Table 3. The results well reflect active cell cycling and high metabolic activity of satellite cells.

Expression of Cell-Cell Adhesion Molecules on Satellite Cells

Both single gene analysis and GSEA suggest that cell-cell adhesion is one of the key elements in the regulation of satellite cells. Preferential expression of the following genes in quiescent satellite cells was confirmed by RT-PCR and quantitative PCR (supplemental online Fig. 1A, 1B): *VE-cadherin* (*cadherin 5*), *Vcam1*, *Icam1*, *Cldn5* (*claudin 5*), *Esam* (*endothelial cell-specific adhesion molecule*), and *Pcdhb9* (*protocadherin beta 9*). To date, several cell surface markers for satellite cells have been identified, including M-cadherin, syndecan3, syndecan4, c-met, Vcam-1, NCAM-1, and CD34 [5, 38–43]. Vascular endothelial (VE)-cadherin, Icam1, claudin5, Esam, and Pcdhb9 should be added to the list. Because *Esam* is upregulated in long-term hematopoietic stem cells and mammary gland side population cells [44, 45], the expression of *Esam* in quiescent satellite cells is quite intriguing. When transverse sections of adult skeletal muscle were stained with specific antibodies, M-cadherin was found at the site of contact between satellite cells and myofibers (supplemental online Fig. 1C) [38]. Vcam-1 and VE-cadherin proteins are also detected at the boundary of satellite cells and myofibers. Although their roles in regulation of satellite cells remain to be determined, our observations suggest that cell-cell adhesion molecules have critical roles in keeping satellite cells in an undifferentiated and quiescent state and in protecting satellite cells from cell death. We also confirmed that FACS with Vcam-1 anti-

Table 1. Gene sets upregulated in quiescent satellite cells and genes with high enrichment scores

	1 − (FDR q value)
Biological process	
Cell-cell adhesion	.791
Tek, Vcam1, Icam2, Cldn5, Cdh5, Icam1	
Regulation of cell growth	.787
Socs3, Htra1, Htra3, Ctgf, Igfbp4, Creg1, Igfbp7, Epc1, Cyr61, Crim1, Nov, Igfbp6, Nedd9	
Transmembrane receptor protein tyrosine phosphatase signaling pathway	.751
Ptprz1, Ptprf, Ptprb, Ptprd, Ptprk, Ptprs, Ptprr	
Cellular component	
Insoluble fraction	.786
Dmd, Dag1, Plec1, Des, Hspb1	
Extracellular region	.766
Sepp1, Htra1, Edn3, Cxcl1, Loxl1, Htra3, Thbs4, Ctgf, Ntf3, Twsg1, Ccl27, Rarres2, Ltbp3, Igfbp4, Apoe, Igf1, Ibsp, Trf, Pthlh, Polydom, Ccl11, Abca3, Thbs3, Wnt4, Pros1, Vwa1, Comp, Nppc, Cyp4v3, Ccl19, Nts, Fbln2, Cocoacrisp, Cxcl2, Igfbp7, C1r, Thbs2, Ccl6, Calca, Cyr61, Icosl, Ccl21c, Crim1, Il6, Degb10, Cxcl9, Csng, C3, Cxcl10, Cxcl14, Inhbb, Il15, Nov, Igfbp6, Mglap, Dkk2, Tnfsf12, Ifnb1, Tfpi2, Cxcl11, Il18, Pi16, Pycard, Lzp-s, Stc1, Lyzs	
Collagen	.766
Col3a1, Col6a2, Col17a1, Col1a2, Col15a1, Col6a3, Col5a3, Col1a1, Col4a1, Col5a1, Col11a1	
Molecular function	
Extracellular matrix structural constituents conferring tensile strength	.774
Col3a1, Col6a2, Col17a1, Col1a2, Col15a1, Col6a3, Col16a1, Col1a1, Col4a1, Col4a5, Col5a1, Col11a1, Col11a2, Col9a1, Col4a2, Col4a4	
Copper ion binding	.764
Aoc3, Cp, Loxl1, Mt1, Atp7a, Heph, Loxl2, Nr1h3	
Lipid transporter activity	.752
Vldlr, Lp1, Apoe, Sorl1, Ldlr, Gpld1, Lrp1	

Gene names are listed according to the rank of enrichment scores. Underlined genes (46/118 genes) are also listed in supplemental online Table 1.
Abbreviation: FDR, false discovery rate.

body efficiently enriches quiescent satellite cells as SM/C-2.6 does (supplemental online Fig. 2).

Calcitonin Receptor Is Sharply Downregulated on Activated Satellite Cells and Reappeared on Renewed Satellite Cells During Muscle Regeneration

RT-PCR verified that CTR is exclusively expressed in quiescent satellite cells but not in activated satellite cells or in nonmyogenic cells (Fig. 3). In addition, we confirmed that calcitonin mRNA is expressed in satellite cells (data not shown). Therefore, we examined the expression of CTR protein in vivo using immunohistochemistry. As shown in Figure 5A, CTR protein was observed in Pax7-positive mononuclear cells beneath the basal lamina in uninjured muscle. We next stained cross-sections of regenerating muscle with anti-CTR antibody. Three days after cardiotoxin injection, many activated satellite cells were stained with anti-M-cadherin antibodies, but CTR expression was not detected on activated satellite cells on the serial sections (Fig. 5B). Furthermore, there were no $Pax7^+/CTR^+$ cells on muscle sections until 7 days after injury (cardiotoxin [CTX]-7d), when $Pax7^+/CTR^+$ cells were again found at the periphery of centrally nucleated, relatively large myofibers but not of small regenerating fibers (Fig. 5C, 5D). The number of $Pax7^+/CTR^+$ cells gradually increased thereafter and reached the level of uninjured muscle by CTX-14d (Fig. 5D). Interestingly, approximately 20% of $Pax7^+/CTR^+$ cells on CTX-7d were found outside the basal lamina (Fig. 5E). This atypical position of satellite cells was transient, and the ratio of satellite cells residing beneath the basal lamina increased during myofiber maturation (data not shown). Taken together, the results suggest that the expression of CTR is found not only on quiescent satellite cells but also on newly formed satellite cells that are closely associated with maturing myofibers.

Calcitonin Inhibits Activation of Quiescent Satellite Cells

To investigate the roles of CTR in the regulation of satellite cells, eel calcitonin, elcatonin, was added to the culture of quiescent satellite cells in vitro before or after activation. Addition of calcitonin before activation significantly inhibited BrdU uptake by quiescent satellite cells (Fig. 6A) but not by already activated satellite cells (Fig. 6A). Interestingly, a short exposure (0.5 hours) to calcitonin was enough to suppress the activation of quiescent satellite cells (Fig. 6B).

MyoD staining of satellite cells revealed that calcitonin/CTR signaling delays the induction of MyoD in quiescent satellite cells (Fig. 6C). The lower percentage of Ki67-positive cells in calcitonin-treated satellite cells also indicated that calcitonin delays the entry of quiescent satellite cells into the cell cycle (Fig. 6C). Calcitonin-treated cells were considerably smaller than control cells on the second day of culture (Fig. 6D), again indicating delayed activation of satellite cells in the presence of calcitonin. A terminal deoxynucleotidyl transferase dUTP nick-end labeling assay excludes the possibility that calcitonin induced apoptosis in satellite cells (Fig. 6E).

To further investigate the effects of calcitonin on activation of quiescent satellite cells, we prepared living single muscle fibers from mouse extensor digitorum longus muscles by using the collagenase digestion method [20] and plated them onto Matrigel-coated 24-well plates at a density of one fiber per well in the presence or absence of calcitonin. In control wells, many satellite cells had detached and migrated from the myofibers 2 days after plating (Fig. 6F). Calcitonin significantly reduced the numbers of satellite cells that had detached from myofibers (Fig. 6F). It was reported that

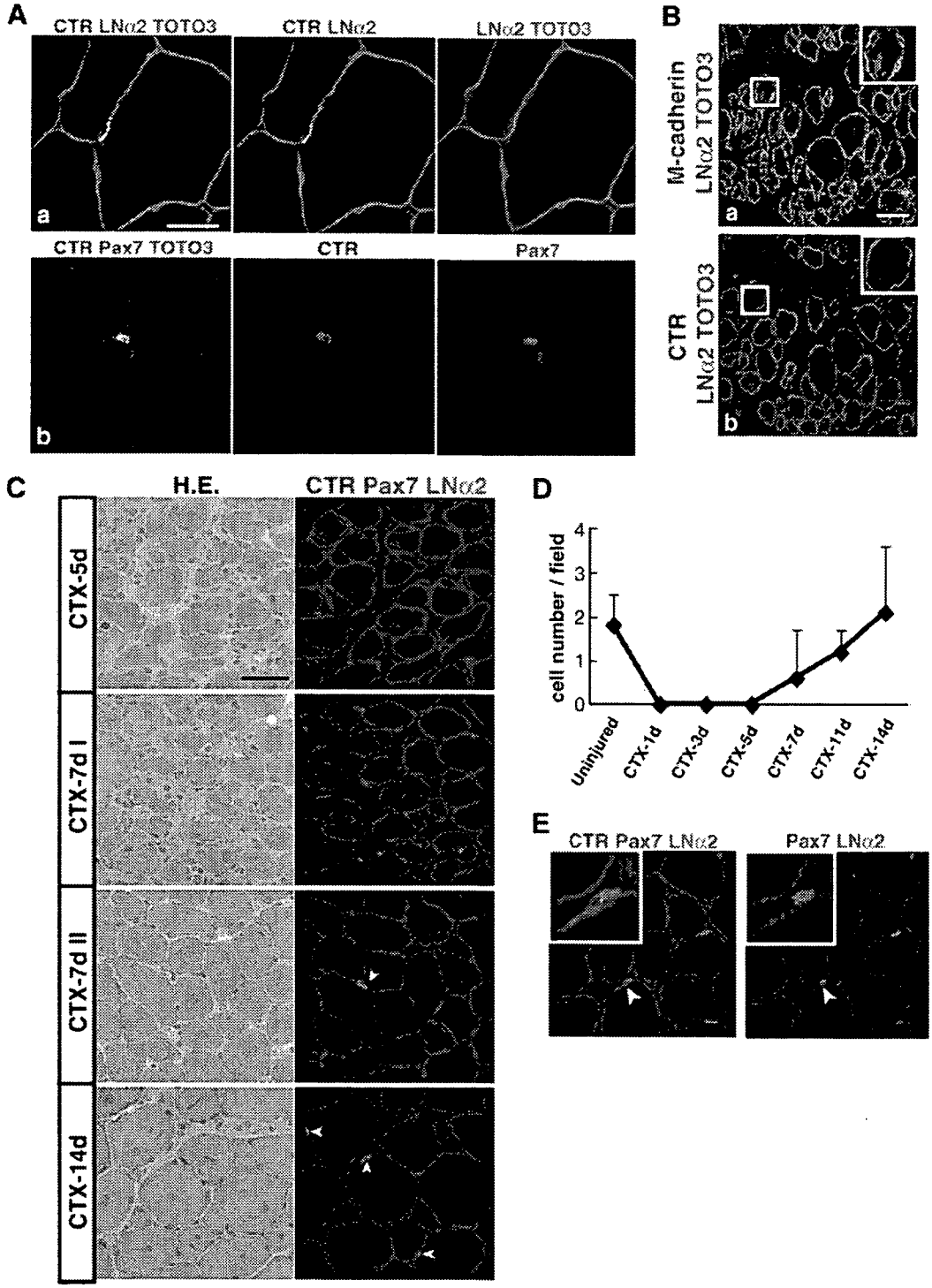

Figure 5. Reappearance of CTR- and Pax7-positive satellite cells in regenerating muscle 7 days after cardiotoxin injection. **(A):** Cross-sections of uninjured skeletal muscle were stained with antibodies to calcitonin receptor (red), laminin $\alpha 2$ chain (green in [Aa]), or Pax7 (green in [Ab]). Nuclei were stained with TOTO3 (blue). Scale bar: 20 μm. **(B):** Three days after CTX injection, regenerating muscles were dissected, and serial cross-sections were stained with antibodies to M-cadherin (red in **[Ba]**) or CTR (red in **[Bb]**) and anti-laminin $\alpha 2$ (green in **[Ba, Bb]**) antibodies. Insets show close-ups of marked areas by white squares. Nuclei were stained with TOTO3 (blue). Scale bar: 40 μm. **(C):** Tibialis anterior muscles were sampled at five (CTX-5d), seven (CTX-7d), and 14 days (CTX-14d) after CTX injection. Sections were coimmunostained with anti-CTR (red), Pax7 (green), and laminin $\alpha 2$ chain (blue) antibodies. Serial sections were stained with H.E. Note that $Pax7^+/CTR^+$ cells were first detected on the seventh day of regeneration around regenerating muscle fibers with a large diameter (CTX-7d II) but not around small-sized fibers (CTX-7d I). Arrowheads indicate CTR-positive Pax7-positive cells. Scale bar: 40 μm. **(D):** Numbers of $Pax7^+/CTR^+$ cells per field at 1, 3, 5, 7, 11, and 14 days after CTX injection. $Pax7^+/CTR^+$ cells were counted in 12–21 randomly selected fields in the regenerating area. The average is shown with SD. **(E):** Cross-sections of regenerating muscle 7 days after CTX injection were coimmunostained with CTR (red), Pax7 (green), and laminin $\alpha 2$ (blue). A typical $Pax7^+/CTR^+$ satellite cell outside the basal lamina is shown (arrowheads). Scale bar: 20 μm. Abbreviations: CTR, calcitonin receptor; CTX, cardiotoxin; d, day; H.E., hematoxylin and eosin; LN$\alpha 2$, laminin $\alpha 2$.

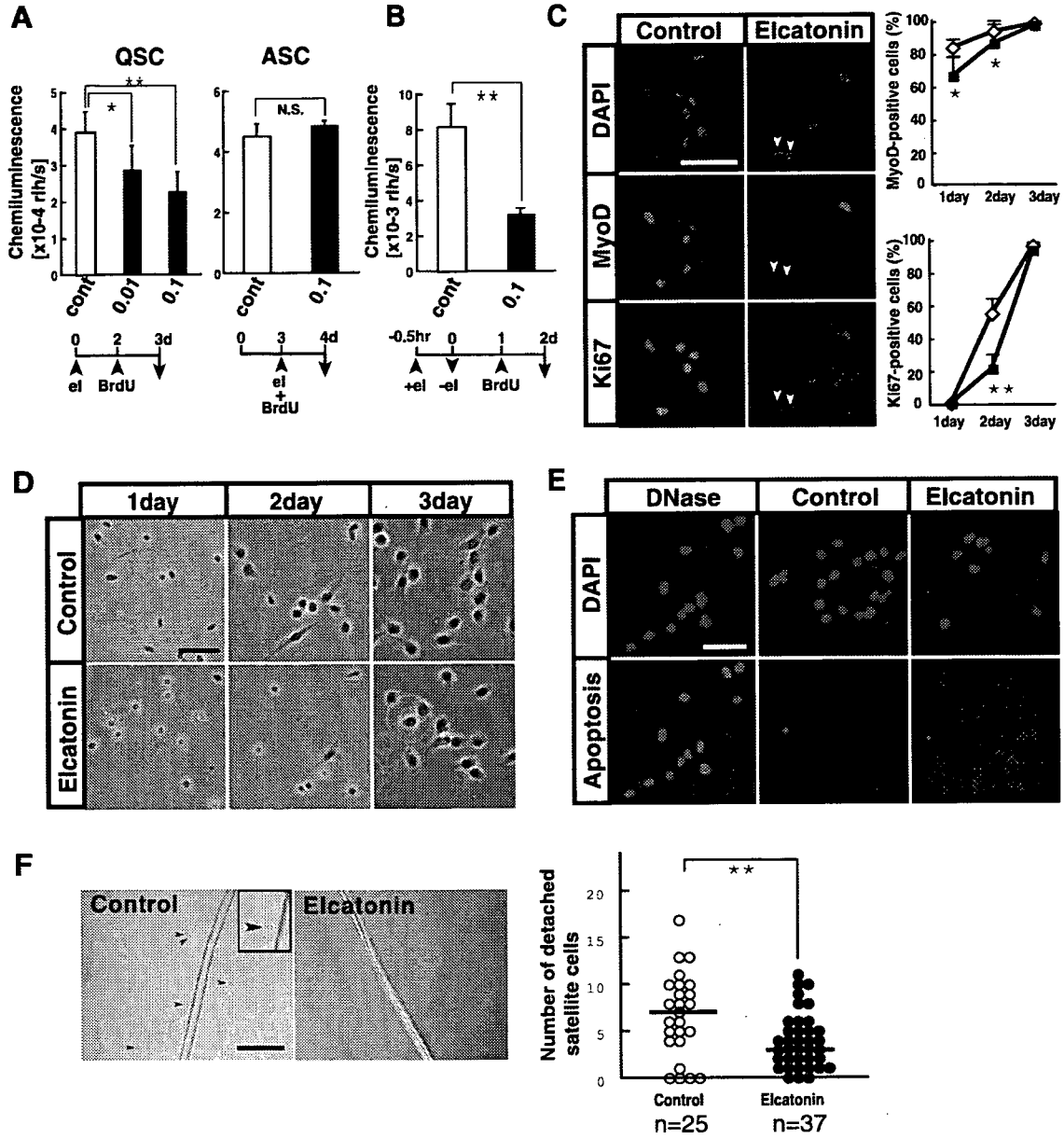

Figure 6. Calcitonin receptor agonist, elcatonin, suppresses activation of quiescent satellite cells. **(A):** Freshly isolated SM/C-2.6$^+$ cells (QSC) and cultured SM/C-2.6$^+$ cells (ASC) were grown in the presence (black) or absence (white) of eel calcitonin, elcatonin. Left: QSC were cultured for 2 days with (0.01 U/ml or 0.1 U/ml) or without elcatonin and then cultured for an additional 24 hours in the presence of BrdU. Right: QSC were cultured for 3 days and then cultured for 24 hours in the presence or absence of elcatonin and BrdU. The vertical axis shows the mean BrdU uptake by satellite cells of three experiments with SD; * $p < .05$, ** $p < .01$ (analysis of variance [ANOVA] test). **(B):** BrdU uptake by QSC exposed to elcatonin for 30 minutes prior to plating. Values are means with SD ($n = 3$); ** $p < .01$. **(C):** QSC cultured in the presence or absence of 0.1 U/ml elcatonin for 2 days were stained with anti-MyoD (red) or Ki67 (green) antibodies. Nuclei were stained with DAPI (blue). Arrowheads indicate MyoD- and Ki67-negative satellite cells. Graphs show the frequency of MyoD- or Ki67-positive cells 1, 2, or 3 days after plating with (closed square) or without (open diamond) elcatonin. More than 100 cells were counted. Values are means with SD; * $p < .05$, ** $p < .01$. Scale bar: 50 μm. **(D):** Phase contrast images of satellite cells 1, 2, and 3 days after plating in the presence or absence of 0.1 U/ml elcatonin. Note that many elcatonin-treated satellite cells are smaller than nontreated cells 2 days after plating. Scale bar: 50 μm. **(E):** Terminal deoxynucleotidyl transferase dUTP nick-end labeling assay on satellite cells cultured with or without elcatonin for 2 days. Apoptotic cells are in red. Nuclei were stained with DAPI (blue). As a positive control, satellite cells were pretreated with DNase. Scale bar: 50 μm. **(F):** Activation of satellite cells on myofibers in vitro. Isolated muscle fibers were plated at a density of one fiber per well and cultured with or without elcatonin (0.1 U/ml) for 2 days, and the numbers of satellite cells that had detached and migrated from each muscle fiber (arrowheads) were counted. Inset is a close-up image of a detached satellite cell. Scale bar: 100 μm. ANOVA t test, ** $p < .01$. Abbreviations: ASC, activated satellite cells; BrdU, 5-bromo-2′-deoxyuridine; d, days; DAPI, 4,6-diamidino-2-phenylindole; el, elcatonin; hr, hours; NS, nonsignificant; QSC, quiescent satellite cells.

calcitonin signaling was mediated via cAMP [46]. An analog of cAMP, dibutyryl cAMP, and an activator of adenylate cyclase, forskolin, also attenuated the activation of satellite cells in vitro (data not shown). Collectively, our results suggest that calcitonin/CTR signaling inhibits activation of satellite cells but not their proliferation or survival. The downstream target molecules of calcitonin/CTR remain to be determined.

CONCLUSION

Single gene-level analysis revealed several candidate genes that negatively regulate cell cycling of satellite cells. Furthermore, our results suggested that satellite cells express both myogenic and antimyogenic molecules to maintain their delicate state.

GSEA showed that dormant satellite cells coordinately express gene groups involved in cell-cell adhesion, cell-extracellular matrix interaction, copper and iron homeostasis, lipid transport, and regulation of cell growth. Although the result shows one aspect of regulation of quiescent satellite cells, more elaborate gene grouping might be needed to further understand the molecular regulation of quiescent satellite cells.

Finally, we showed that calcitonin receptor is specifically expressed on quiescent satellite cells and transmits signals that attenuate the entry of quiescent satellite cells into the cell cycle. Our results would greatly facilitate the investigation of molecular regulation of satellite cells in both physiological and pathological conditions.

ACKNOWLEDGMENTS

This work was supported by Grants for Research on Nervous and Mental Disorders (16B-2), Health Science Research Grants for Research on the Human Genome and Gene Therapy (H16-genome-003), for Research on Brain Science (H15-Brain-021) from the Japanese Ministry of Health, Labor and Welfare, Grants-in-Aids for Scientific Research (14657158, 153,90281, and 165,90333) from the Japanese Ministry of Education, Culture, Sports, Science and Technology, and "Ground-Based Research Program for Space Utilization" promoted by Japan Space Forum.

DISCLOSURE OF POTENTIAL CONFLICTS OF INTEREST

The authors indicate no potential conflicts of interest.

REFERENCES

1 Bischoff R. Analysis of muscle regeneration using single myofibers in culture. Med Sci Sports Exerc 1989;21(suppl 5):S164–S172.
2 Partridge T. Reenthronement of the muscle satellite cell. Cell 2004;119: 447–448.
3 Mauro A. Satellite cell of skeletal muscle fibers. J Biophys Biochem Cytol 1961;9:493–495.
4 Schultz E, Gibson MC, Champion T. Satellite cells are mitotically quiescent in mature mouse muscle: an EM and radioautographic study. J Exp Zool 1978;206:451–456.
5 Cornelison DD, Wold BJ. Single-cell analysis of regulatory gene expression in quiescent and activated mouse skeletal muscle satellite cells. Dev Biol 1997;191:270–283.
6 Bischoff R. Satellite and stem cells in muscle regeneration. In: Engel AG, Franzini-Armstrong C, eds. Myology. Vol 1. New York: McGraw-Hill, 2004:66–86.
7 Collins CA, Olsen I, Zammit PS et al. Stem cell function, self-renewal, and behavioral heterogeneity of cells from the adult muscle satellite cell niche. Cell 2005;122:289–301.
8 Seale P, Sabourin LA, Girgis-Gabardo A et al. Pax7 is required for the specification of myogenic satellite cells. Cell 2000;102:777–786.
9 Grounds MD, Yablonka-Reuveni Z. Molecular and cell biology of skeletal muscle regeneration. Mol Cell Biol Hum Dis Ser 1993;3: 210–256.
10 Wagers AJ, Conboy IM. Cellular and molecular signatures of muscle regeneration: Current concepts and controversies in adult myogenesis. Cell 2005;122:659–667.
11 Asakura A, Komaki M, Rudnicki M. Muscle satellite cells are multipotential stem cells that exhibit myogenic, osteogenic, and adipogenic differentiation. Differentiation 2001;68:245–253.
12 Wada MR, Inagawa-Ogashiwa M, Shimizu S et al. Generation of different fates from multipotent muscle stem cells. Development 2002;129: 2987–2995.
13 Shefer G, Wleklinski-Lee M, Yablonka-Reuveni Z. Skeletal muscle satellite cells can spontaneously enter an alternative mesenchymal pathway. J Cell Sci 2004;117:5393–5404.
14 McCroskery S, Thomas M, Maxwell L et al. Myostatin negatively regulates satellite cell activation and self-renewal. J Cell Biol 2003;162: 1135–1147.
15 Thomas M, Langley B, Berry C et al. Myostatin, a negative regulator of muscle growth, functions by inhibiting myoblast proliferation. J Biol Chem 2000;275:40235–40243.
16 Cao Y, Zhao Z, Gruszczynska-Biegala J et al. Role of metalloprotease disintegrin ADAM12 in determination of quiescent reserve cells during myogenic differentiation in vitro. Mol Cell Biol 2003;23: 6725–6738.
17 Carnac G, Fajas L, L'Honore A et al. The retinoblastoma-like protein p130 is involved in the determination of reserve cells in differentiating myoblasts. Curr Biol 2000;10:543–546.
18 Fukada S, Higuchi S, Segawa M et al. Purification and cell-surface marker characterization of quiescent satellite cells from murine skeletal muscle by a novel monoclonal antibody. Exp Cell Res 2004;296: 245–255.
19 Uezumi A, Ojima K, Fukada S et al. Functional heterogeneity of side population cells in skeletal muscle. Biochem Biophys Res Commun 2006;341:864–873.
20 Rosenblatt JD, Lunt AI, Parry DJ et al. Culturing satellite cells from living single muscle fiber explants. In Vitro Cell Dev Biol Anim 1995; 31:773–779.
21 Ojima K, Uezumi A, Miyoshi H et al. Mac-1(low) early myeloid cells in the bone marrow-derived SP fraction migrate into injured skeletal muscle and participate in muscle regeneration. Biochem Biophys Res Commun 2004;321:1050–1061.
22 Mootha VK, Lindgren CM, Eriksson KF et al. PGC-1alpha-responsive genes involved in oxidative phosphorylation are coordinately downregulated in human diabetes. Nat Genet 2003;34:267–273.
23 Ashburner M, Ball CA, Blake JA et al. Gene ontology: Tool for the unification of biology. The Gene Ontology Consortium. Nat Genet 2000;25:25–29.
24 Holyoake T, Jiang X, Eaves C et al. Isolation of a highly quiescent subpopulation of primitive leukemic cells in chronic myeloid leukemia. Blood 1999;94:2056–2064.
25 Missero C, Calautti E, Eckner R et al. Involvement of the cell-cycle inhibitor Cip1/WAF1 and the E1A-associated p300 protein in terminal differentiation. Proc Natl Acad Sci U S A 1995;92:5451–5455.
26 Zhang P, Wong C, Liu D et al. p21(CIP1) and p57(KIP2) control muscle differentiation at the myogenin step. Genes Dev 1999;13:213–224.
27 Cooper RN, Tajbakhsh S, Mouly V et al. In vivo satellite cell activation via Myf5 and MyoD in regenerating mouse skeletal muscle. J Cell Sci 1999;112:2895–2901.
28 Reshef R, Maroto M, Lassar AB. Regulation of dorsal somitic cell fates: BMPs and Noggin control the timing and pattern of myogenic regulator expression. Genes Dev 1998;12:290–303.
29 Dahlqvist C, Blokzijl A, Chapman G et al. Functional Notch signaling is required for BMP4-induced inhibition of myogenic differentiation. Development 2003;130:6089–6099.
30 Kuroda K, Tani S, Tamura K et al. Delta-induced Notch signaling mediated by RBP-J inhibits MyoD expression and myogenesis. J Biol Chem 1999;274:7238–7244.
31 Conboy IM, Rando TA. The regulation of Notch signaling controls satellite cell activation and cell fate determination in postnatal myogenesis. Dev Cell 2002;3:397–409.
32 Conboy IM, Conboy MJ, Smythe GM et al. Notch-mediated restoration of regenerative potential to aged muscle. Science 2003;302: 1575–1577.
33 Lu J, Webb R, Richardson JA et al. MyoR: A muscle-restricted basic helix-loop-helix transcription factor that antagonizes the actions of MyoD. Proc Natl Acad Sci U S A 1999;96:552–557.
34 Zhao P, Hoffman EP. Musculin isoforms and repression of MyoD in muscle regeneration. Biochem Biophys Res Commun 2006;342: 835–842.
35 Gustafsson MK, Pan H, Pinney DF et al. Myf5 is a direct target of long-range Shh signaling and Gli regulation for muscle specification. Genes Dev 2002;16:114–126.
36 Mankoo BS, Skuntz S, Harrigan I et al. The concerted action of Meox homeobox genes is required upstream of genetic pathways essential for the formation, patterning and differentiation of somites. Development 2003;130:4655–4664.

37 Zhou XH, Brandau O, Feng K et al. The murine Ten-m/Odz genes show distinct but overlapping expression patterns during development and in adult brain. Gene Expr Patterns 2003;3:397–405.
38 Irintchev A, Zeschnigk M, Starzinski-Powitz A et al. Expression pattern of M-cadherin in normal, denervated, and regenerating mouse muscles. Dev Dyn 1994;199:326–337.
39 Cornelison DD, Filla MS, Stanley HM et al. Syndecan-3 and syndecan-4 specifically mark skeletal muscle satellite cells and are implicated in satellite cell maintenance and muscle regeneration. Dev Biol 2001;239: 79–94.
40 Beauchamp JR, Heslop L, Yu DS et al. Expression of CD34 and Myf5 defines the majority of quiescent adult skeletal muscle satellite cells. J Cell Biol 2000;151:1221–1234.
41 Jesse TL, LaChance R, Iademarco MF et al. Interferon regulatory factor-2 is a transcriptional activator in muscle where It regulates expression of vascular cell adhesion molecule-1. J Cell Biol 1998; 140:1265–1276.
42 Illa I, Leon-Monzon M, Dalakas MC. Regenerating and denervated human muscle fibers and satellite cells express neural cell adhesion molecule recognized by monoclonal antibodies to natural killer cells. Ann Neurol 1992;31:46–52.
43 Charge SB, Rudnicki MA. Cellular and molecular regulation of muscle regeneration. Physiol Rev 2004;84:209–238.
44 Forsberg EC, Prohaska SS, Katzman S et al. Differential expression of novel potential regulators in hematopoietic stem cells. PLoS Genet 2005;1:e28.
45 Behbod F, Xian W, Shaw CA et al. Transcriptional profiling of mammary gland side population cells. STEM CELLS 2006;24:1065–1074.
46 Becker K, Muller B, Nylen E et al. Calcitonin Gene Family of Peptides. Vol 1. 2nd ed. New York: Academic Press, 2002.

See www.StemCells.com for supplemental material available online.